

# Experimental determination of the laminar burning velocity of methane-oxygen-flames stabilized with cylindrical burners at various preheating temperatures

P. Schlinger<sup>\*1</sup>, W. Jazkow<sup>1</sup>, C. Weis<sup>1</sup>, P. Habisreuther<sup>1</sup>, B. Stelzner<sup>1</sup>, D. Trimis<sup>1</sup>

<sup>1</sup>Engler-Bunte-Institute Combustion Technology, Karlsruhe Institute of Technology, Karlsruhe, Germany

## Abstract

The laminar burning velocity of pure methane-oxygen flames stabilized with a cylindrical tube burner was determined experimentally via optical methods (Schlieren-technique and CH\* chemiluminescence). Both flow exit profiles were examined: a fully developed and a plug flow profile. The experiments were conducted for an equivalence ratio range of  $0.5 < \Phi < 2.2$ , while the inlet temperature of the educts was set to 293 K. The results of the CH<sub>4</sub>-O<sub>2</sub> flames show a maximum laminar burning velocity of approx. 360 cm/s near stoichiometric conditions.

## Introduction

The application of pure oxygen as an oxidizer in combustion processes offers several advantages: in addition to an increased temperature compared to conventional air flames due to a reduced thermal ballast in the form of missing nitrogen, the combustion of fuels with pure oxygen produces a flue gas of high purity. The high purity of the flue gases enables an easier separation of the flue gases in order to e.g. effectively reduce otherwise occurring greenhouse gas emissions like CO<sub>2</sub>, or to produce a particularly pure synthesis gas.

An increased temperature enables a more efficient use of the fuel, since the heat transfer can be increased due to the increased differential temperature, which in turn can lead to a reduced use of fuel and thus a reduced emission of greenhouse gases like CO<sub>2</sub>. However, the increased temperature also leads to an increased laminar burning velocity, which is why fuel-rich methane oxygen flames are of high interest for the chemical industry. The burner design and process control may have to be adjusted, which is why the laminar burning velocity was determined in this study.

Due to its fundamental nature, the laminar burning velocity has been studied by various researchers thoroughly for different fuel-oxidizer combinations via different methods. Unfortunately, only few data exist for the laminar burning velocity of pure methane-oxygen flames stabilized on cylindrical burners (Bunsen type burner). Very early studies go back to Jahn, who determined the laminar burning velocity in a Bunsen burner over a wide range as early as 1932 [1].

In 2009, Dong et al. studied the laminar burning velocity of H<sub>2</sub>, CO, and H<sub>2</sub>/CO air flames in a Bunsen burner. Contrary to the definition of laminar burning velocity, which is the perpendicular component of the relative velocity between the flame front and the fresh gas, they used the area of the reaction zone instead of the area of the unburned flame zone for their calculations. Their results are nevertheless consistent with those of previous studies and numerical simulations, which in turn justifies their method [2].

Also in 2009, Mazas et al. studied the laminar burning velocity in premixed methane with oxygen-

enriched air flames, to which water vapor was added, under moderate preheating. They used a cylindrical tube burner and applied Schlieren-technique to demonstrate the thermodynamic influence of water vapor on the laminar burning velocity [3].

In 2012, Oh et al. studied the laminar burning velocity of pure methane-oxygen mixtures using a cylindrical tube burner. They used both the Schlieren-technique and recorded CH\*-chemiluminescence from the flame front and used it for further calculations. Both techniques have shown good accordance, although the results do not quite match their previously performed numerical calculations [4].

In 2016, Shang et al. determined the laminar burning velocity of H<sub>2</sub>/CO/air mixtures at a Bunsen burner using Schlieren-technique and chemiluminescence. In an extended data analysis, they were able to eliminate the influence of flame stretch on the laminar burning velocity from the measured data via a nonlinear extrapolation. Their results are in good agreement with results from stretch-corrected spherical flame and counter-flow flame methods [5].

## Numerical approach

For the present study, numerical calculations were performed beforehand using the PREMIX package of the Chemkin program (originally developed by Kee et al.) on burners stabilized flames for premixed gas mixtures [6,7]. Eight different mechanisms were used, representing detailed reaction chemistry. The key variation parameter was the fuel oxidizer mixture: its composition was varied between an equivalence ratio of 0.5 and 3.33. An overview for the used mechanisms is shown in Table 1.

**Table 1: Overview for used mechanisms.**

mechanism	chain-length	# species	# of reactions	ref.
Caltech 2.3	C16	192	1156	[8]
GRI 3.0	C3	53	325	[9]
ABF	C16	101	544	[10]
USC/II	C7	111	784	[11]
DLR	C16	189	1327	[12]
HPMech3.3	C6	92	615	[13]
FFCM1	C2	38	291	[14]
Aramco 1.3	C3	124	766	[15]

\* Corresponding author: [Paul.Schlinger@partner.kit.edu](mailto:Paul.Schlinger@partner.kit.edu)  
Proceedings of the European Combustion Meeting 2023

## Experimental approach

To determine the laminar burning velocity of on cylindrical burners stabilized flames, two flow profiles of the fresh gas are desired: either a fully developed laminar flow profile or a flow profile that is constant over the cross section (plug-flow profile). Both profile variants lead to a different visual appearance and deviate to varying degrees from the shape of a perfect cone. While the tube flow (fully developed flow) has a velocity of almost zero near the tube wall, which leads to a strong curvature in the flame edges, the centre of the flame (flame tip) in both fully developed and plug-flow profile is characterized by combustion anomalies in the tip and therefore fluctuates there. By stabilizing the flame with a tube or nozzle, heat is transferred from the flame to the tube/nozzle. These heat losses can lead to a reduced local laminar burning velocity. It is therefore obvious that tubes with a larger inner diameter are preferred, since at a constant outlet velocity the mass flow rate increases in square with the internal diameter, whereas the stabilising effect of cylindrical burners only increases linearly with the inner diameter. However, an increasing inner diameter also leads to a linearly increasing Reynolds number, so that it must be ensured that a laminar flow is investigated. In combination with the expected laminar burning velocity from the preliminary numerical investigations, it is therefore necessary to select the inner diameter such that the widest possible operating range can be investigated. Due to the wide range of laminar burning velocity of pure  $\text{CH}_4\text{-O}_2$  flames, it is necessary to provide a wide range of flow velocities. The difficulty is that due to the high laminar burning velocity near stoichiometric composition, the flow velocity remains laminar for the entire bandwidth only for smaller tube diameters (cf. Figure 3). Therefore, only results obtained with the 2 mm tube and nozzle are presented for  $\text{CH}_4\text{-O}_2$  flames in this study.

One challenge in determining the laminar burning velocity with the Bunsen burner method is that the optical shape of the flame cone is used. However, the laminar burning velocity is defined as the normal velocity component of the fresh gas flow, while the visible flame cone in the form of chemiluminescence only results from the increased temperature due to the released heat within the flame. As a result, the laminar burning velocity is usually underestimated because the flame surface is larger than the area of the fresh gas flowing through it. A commonly used radical as a marker is the  $\text{CH}^*$  radical, as it is mainly formed within the flame front and is therefore suitable as a marker for determining the flame front, which is why  $\text{CH}^*$  chemiluminescence was recorded in this work. Another possibility is the Schlieren-technique. Here, parallel light is used to visualise the density gradient within the flame front. Since the density within the flame structure changes mainly in the reaction zone, it is even closer to the area of the fresh gas cone compared to  $\text{CH}^*$ -chemiluminescence. Therefore, the Schlieren-technique is even better suited to determine

the laminar burning velocity, which is why it was used simultaneously in this work.

## Experimental setup

The testing rig can be divided into three sections: optical setup, gas supply and burner (see Figure 1 and Figure 2). The burner section consists of a stainless-steel tube with an inner diameter of 100 mm, into which interchangeable cylindrical tubes of different diameters (2 mm, 4 mm, 6 mm, 8 mm and 10 mm inner diameter) could be centrally and coaxially installed. All tube tips were pointed to reduce heat transfer from the stabilized flame into the tubes. Besides mounting the used tube, the outer tube allowed a co-flow to be supplied to increase the stabilisation of the flames if necessary.

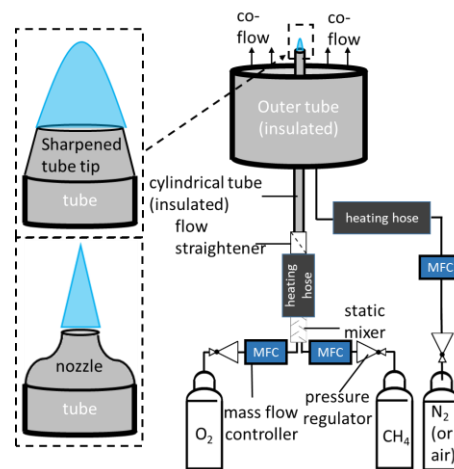


Figure 1: Schematic representation of the burner setup.

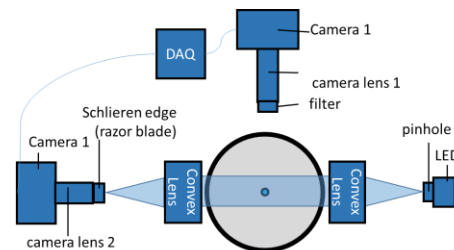


Figure 2: Schematic representation of the optical setup.

The gas supply line was designed so that methane and oxygen were supplied from gas cylinders via pressure reducers with thermal mass flow controllers (Bronkhorst high-Tech BV). These were brought together in a T-piece and then homogeneously mixed in a downstream static mixing module (Kenics<sup>TM</sup>). Subsequently, the fresh gas mixture was conditioned via a controlled heating hose (Horst GmbH) and passed through a filter element (mesh size  $7\ \mu\text{m}$ ) to homogenize the flow. Subsequently, the fuel-oxidizer mixture was passed through a 400 mm long cylindrical tube to the tube outlet to obtain a fully developed laminar flow profile (ratio from length/diameter  $> 40$ ). In order to investigate the influence of different flow profiles, a Mache-Hebra nozzle (according to

DIN ISO EN 5167) was mounted on to the 10 mm tube, reducing the inner diameter from 10 mm to 2 mm to establish a plug flow profile. The temperature of the unburned fresh gas was controlled and adjusted by means of a type-K thermometer. The co-flow was fed with compressed air and was heated to the educts temperature by a heating hose to minimize heat losses. The outer jacket of the outer tube was heated with heating cords (Horst GmbH) and additionally insulated in several layers to reduce further heat losses. The optical setup consisted of the following components: a.) chemiluminescence: a CMOS-camera (Bluefox mv3 BF3-1020G) with spacer ring (f-#/2.3, focal-length: 50 mm, spatial resolution: ~44 px/mm). An upstream optical filter ensured that only the chemiluminescence of the CH\* radical was recorded, as it is suitable as an indicator for the flame zone (CWL = 430 nm, FWHM = 10 nm). The setup of the Schlieren-technique consisted of the following components: high power LED (Thorlabs GmbH), precision pinhole (d = 500  $\mu$ m), two plano-convex lenses (d = 100 mm, focal length: 400 mm), high precision manipulator with razor-blade and an CCD-camera (Bluefox mv3 BF-223G) with camera objective (f-#/2.5, focal-length: 75 mm, spatial resolution: ~44 px/mm). Using the high-power LED and pinhole, a point light source was artificially created and positioned at the focal point of the first lens with to parallelize the light. The light then passed through the burner section and was partially deflected by the density gradient within the flame zone.

The second lens refocused the undeflected light to a point where exactly the razor blade was positioned horizontally as a sharp edge. As a result, the light deflected by the flame zone was no longer captured by the camera and thus the area of the flame where the highest density change occurs was visible (negative representation of the flame zone). For each operating point, 50 images were recorded at a frequency of 30 Hz. The exposure time of each operating point was set individually to maintain an equal intensity distribution. For each image, the laminar burning velocity was calculated individually, checked for plausibility and afterwards averaged.

The operating points were determined in advance based on the results of the previously conducted numerical calculations. In order to stabilise sufficiently high flames, the volume flows were set as a function of equivalence ratio.

It was considered that the flow must be laminar, so that the Reynolds number was calculated as a function of the operating point and inner tube diameters. Therefore, the tube and the Mache-Hebra nozzle with an inner diameter of 2 mm were used for the experiments with CH<sub>4</sub>-O<sub>2</sub> (compare with Figure 9 and Figure 10).

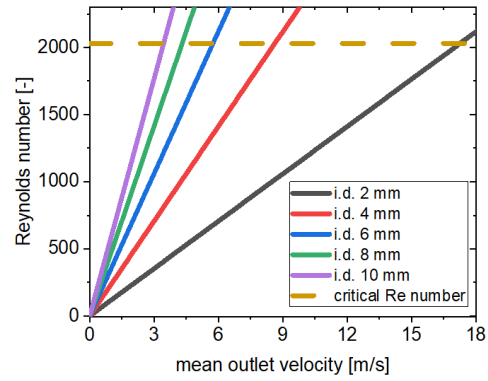


**Figure 3: Critical mean outlet velocities depending on the burner tube inner diameter.**

The flame is stabilised at the tip of the tube burner. However, the flame does not resemble a perfect cone and underlies local stretch and curvature, especially near the burner rim and at the flame tip. Those effects have to be considered. A schematic overview of a stabilised flame is shown in Figure 6. The laminar burning velocity is the velocity at which the unstretched flame front moves perpendicularly toward the unburned mixture and is depicted as  $s_L$ .

There are several ways to derive the laminar burning velocity from the images for the particular gas mixture. Since the premixed gas must flow through both the flame front and the tube exit, it is suitable to derive a mass balance:

$$\dot{m} = \rho_u A_F s_L, \quad \text{equation 1}$$

where  $\dot{m}$  describes the mass flow,  $\rho_u$  is the density of the unburned gas mixture and  $A_F$  is the flame surface. Since the same mass flow exits the cylindrical tube, it can be expressed as follows:

$$\dot{m} = \rho_u A_0 u_0, \quad \text{equation 2}$$

where  $A_0$  is the outlet area of the cylindrical tube and  $u_0$  is the average outlet velocity of the unburned gas mixture. With equation 1 and equation 2, this leads to:

$$s_{L,area} = \frac{A_0}{A_F} u_0, \quad \text{equation 3}$$

This is the equation used to calculate the laminar burning velocity according to the so-called ‘‘area method’’. Since the measured area is larger, than the area of the fresh-gas cone, this method is somewhat subject to error.

For an axisymmetric and steady flame, the laminar burning velocity can also be determined with the ‘‘angle method’’. In this approach, it is assumed that the laminar burning velocity is equal to the normal component of the velocity of the unburned gas mixture exiting the tube. With the half-cone angle  $\alpha$ , measured between the flame front and the centre line of the axisymmetric flame, this leads to the following equation 4:

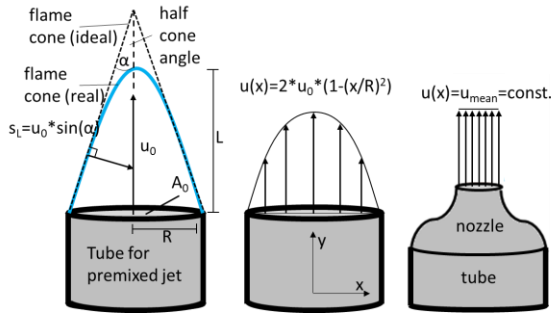


Figure 4: Schematic overview of a stabilized flame.

$$s_{L,angle} = u_0 \sin(\alpha), \quad \text{equation 4}$$

which is used to calculate the laminar burning velocity according to the so-called “angle method”. For flames with large curvature, it is suitable to determine a mean angle where it is reasonably constant. As mentioned

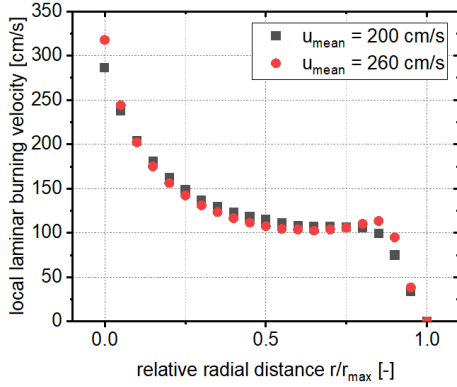


Figure 5: Local laminar burning velocities for  $\text{CH}_4\text{-O}_2$  flames ( $\Phi = 2.0$ ) considering the parabolic velocity distribution according to Hagen-Poiseuille.

before this method is flawed due to the stretch and curvature of the flame at the tip and area near the rim of the tube.

Another suitable method to derive the laminar burning velocity is based on a correlation of flame height and tube diameter. For the geometrical characteristics, it can be deduced, that the flame contour can be described as follows [16]:

$$\frac{dx}{dy} = \sqrt{\left(\frac{u_0}{s_L}\right)^2 - 1}, \quad \text{equation 5}$$

which for  $u_0 \gg s_L$  becomes:

$$s_{L,height} \approx u_0 \frac{R}{L}, \quad \text{equation 6}$$

where  $R$  describes the tube radius and  $L$  the flame height. The method using this correlation is known as the “height method”. This correlation is valid, if the gas outlet velocity is homogeneous (plug flow profile). Since the velocity distribution of a fully developed flow in a tube is parabolically distributed according to Hagen-Poiseuille, this must be considered, which leads to the following equation:

$$s_{L,height} \approx u_0 \frac{4R}{3L}. \quad \text{equation 7}$$

As with the aforementioned methods, the “height method” also includes a certain error due to stretch and curvature in the flame tip and thus a differing flame height.

Considering the parabolic velocity distribution of the gas mixture at the tube outlet, the laminar burning velocity can be approximated by calculating the local laminar burning velocity. For this purpose, it is necessary to determine the local angle of the flame front in increments and to multiply their sinusoidal values by the corresponding velocities from the velocity distribution according to Hagen-Poiseuille [16]. An exemplary plot of the local laminar burning velocity for two flames versus the radial distance is shown in Figure 5.

The local laminar burning velocity exceeds the laminar burning velocity near the centre line and decreases continuously with further distance to the centre line until it reaches a certain plateau, where the product of the sine of the local angle and the local velocity is almost constant. With further distance from the centreline, the local laminar burning velocity decreases. The value of the constant plateau is then used as laminar burning velocity. This method is further referred to as the “Hagen-Poiseuille method”.

### Evaluation procedure

In the first step, the images were cropped to the flame area to reduce unnecessary data and the intensity was normalized to facilitate the edge detection. The images are an integral image of an axisymmetric 3D flame, requiring an Abel-inversion to reconstruct the true position of the flame front in the form of a 2D structure. A comparison of Abel-inverted and non-Abel-inverted images showed that the position of the maximum intensity in the integral image coincides with the position of the 2D flame structure, which is why Abel-inversion was not used further.

A custom edge detection algorithm was applied to detect the inner edge of the flame front, the flame tip and the base of the flame. In the case of the tube flames, the inner edge was then approximated using a 5<sup>th</sup> degree polynomial fit. In case of nozzle flames, a linear fit was applied. An exemplary procedure for tube flames is shown in Figure 6 (inner diameter: 2 mm,  $\text{CH}_4\text{-O}_2$ :  $\Phi = 1.0$ ).

### Preliminary investigation

To validate the measurement technique via chemiluminescence, methane-air flames stabilised on a 10 mm tube were analysed and the results were compared by the different methods with data from literature (compare Figure 7) [17]. In general, all series of measurements have a similar shape. In the case for the angle method, it is evident that the method deviates strongly from the literature data. Therefore, the method for tube flames was not investigated further.

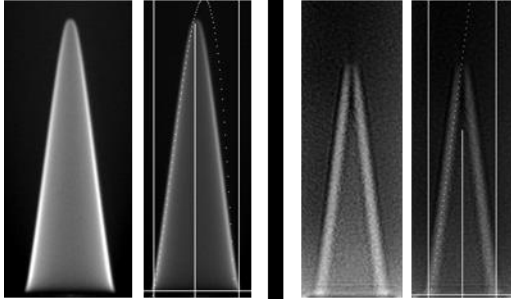


**Figure 6: Procedure of the post-processing, CH<sub>4</sub>-O<sub>2</sub> ( $\Phi = 2.0$ , standard inlet conditions,  $d = 2$  mm), left: chemiluminescence and tube flame, right: Schlieren-technique and nozzle flame.**

The area method, on the other hand, is closer to the literature data, but still deviates remarkably. One possible explanation is that the recorded CH\*-chemiluminescence lies within the flame front, so that the determined area exceeds the surface area of the flame front, and thus the laminar burning velocity is slightly underestimated. The height method, similar to the other methods, is slightly too low, which could be explained by curvature, since the flame tip deviates from a perfect cone. The Hagen-Poiseuille method shows the best agreement with literature data over the entire range of examined equivalence ratios. Therefore, it was used for determining the laminar burning velocity of tube flames via CH\*-chemiluminescence in this work.

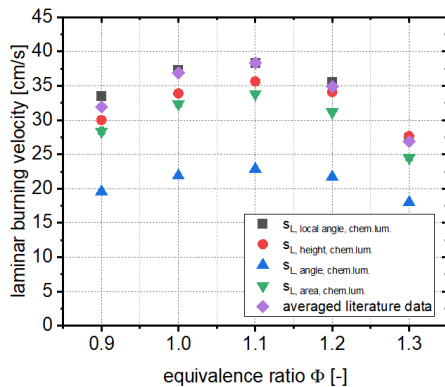


**Figure 7: laminar burning velocity of CH<sub>4</sub>-air flames stabilized on a 10 mm tube burner (chemiluminescence).**

To validate the Schlieren-technique, the obtained images of the aforementioned flames have been compared with literature data (compare Figure 8). As discussed before, all series of measurements have a similar shape. Here, the angle method as well shows a noticeably lower value, which is why the method was not used further. The other three methods are closer to the literature data, whereby the area-method shows the best agreement, which is why it was used for the determination of the laminar burning velocity via Schlieren-technique.

## Results and discussion

Figure 9 shows the laminar burning for flames stabilised on nozzle and tube burners with a constant

ratio of outlet velocity to expected laminar burning velocity of three ( $u/S_L = 3.0$ ) as a function of the equivalence ratio using chemiluminescence.

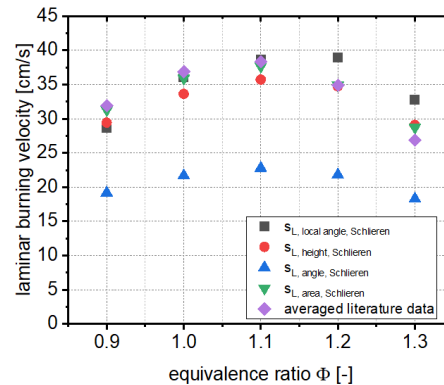


**Figure 8: laminar burning velocity of CH<sub>4</sub>-air flames stabilized on a 10 mm tube burner (Schlieren-technique).**

It can be seen that both measurement series have a similar course and have their maximum around  $\Phi = 0.9$ . The values measured with nozzle flames are lower here over the entire bandwidth, which is about 5%, and are thus lower than those of the tube flames. Figure 10 shows the laminar burning velocities for flames stabilised on nozzle and tube burners with a constant ratio of outlet velocity to laminar burning velocity of three ( $u/S_L = 3.0$ ) as a function of the equivalence ratio using Schlieren-technique. It can be seen that both measurement series have a similar course and have their maximum around  $\Phi = 0.9$ . The nozzle flames deliver values that are about 5% lower near stoichiometric composition, whereby the two values are converging for fuel-rich compositions and the Schlieren-technique even exceeds the chemiluminescence. A comparison of laminar burning velocities with experimental data is shown in Figure 11. The general curve is similar to Jahn's results, and for fuel-rich compositions, there is also good agreement. However, between  $0.5 < \Phi < 2.2$  the data obtained in this work are higher by up to 10%, with the maximum found around  $\Phi = 0.9$  in both cases. Comparison with Oh's results shows a strong discrepancy: on the one hand, the results differ by up to about 35%, with a similar shape for fuel-rich compositions. In this results, however, the maximum is found already around  $\Phi = 1.1$ , while the data from experimental and numerical studies have all found a maximum at around  $\Phi = 0.9$  (compare Figure 11 and Figure 12). The rapid decrease of the results after the maximum differs also from the results obtained in this work. A comparison of the laminar burning velocities with the numerical results is presented in Figure 12. The numerical results show a large deviation in an equivalence ratio range of  $0.5 < \Phi < 1.5$ . The experimental results show a good agreement under lean and fuel-rich conditions, but a higher burning velocity was found near the stoichiometry than in all calculations. However, the maximum is around an equivalence ratio of  $\Phi = 0.9$ .

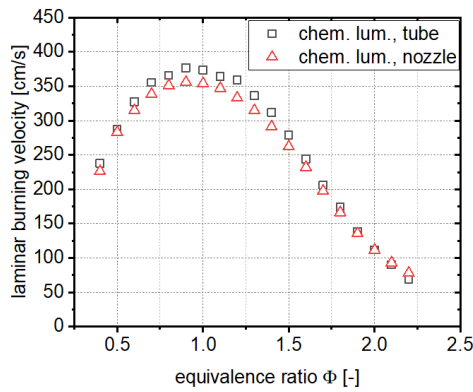


**Figure 9: Laminar burning velocity for CH<sub>4</sub>-O<sub>2</sub> via CH\*-chemiluminescence.**

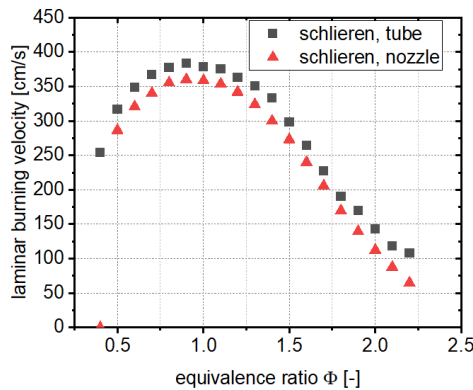


**Figure 10: Laminar burning velocity for CH<sub>4</sub>-O<sub>2</sub> via Schlieren-technique.**

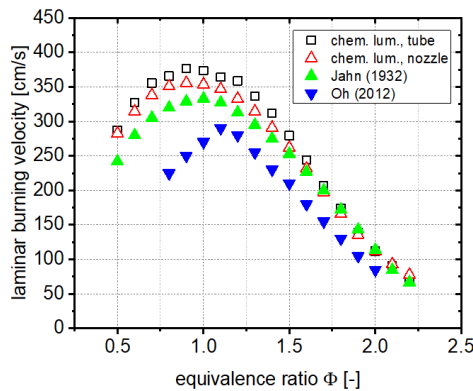


**Figure 11: Comparison with literature data (chemiluminescence).**

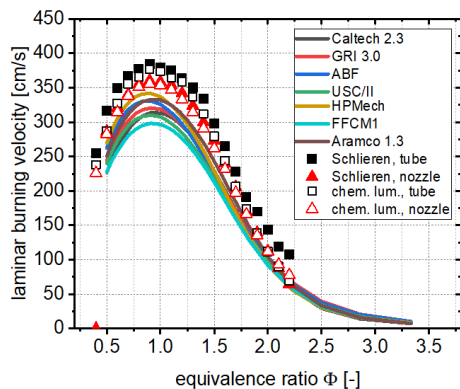


**Figure 12: Comparison with numerical results.**

## Conclusion

The laminar burning velocity for CH<sub>4</sub>-O<sub>2</sub> mixtures was investigated with a tube burner. The equivalence ratio was varied from  $0.5 < \Phi < 2.2$  and the inlet temperature was set at 293 K. Two different burner types (tube with fully developed flow profile and Mache-Hebra nozzle with plug-flow profile) were examined and the flames were recorded with two different measurement techniques (CH\*-chemiluminescence and Schlieren-technique). The results show a value of approximately 360 cm/s near stoichiometry at standard inlet conditions stabilised on nozzle, measured via Schlieren-technique.

## References

- Jahn G (1932) Die Theorie der Zündgeschwindigkeit: unter Berücksichtigung der modernen Reaktionskinetik. Dissertation, Technische Hochschule "Fridericiana" zu Karlsruhe
- Dong C, Zhou Q, Zhao Q et al. (2009) Experimental study on the laminar flame speed of hydrogen/carbon monoxide/air mixtures. *Fuel* 88:1858–1863. <https://doi.org/10.1016/j.fuel.2009.04.024>
- A. Mazas (ed) (2009) Effects of water vapor addition on the laminar burning velocity of methane oxygen-enhanced flames at atmospheric pressure
- Oh J, Noh D (2012) Laminar burning velocity of oxy-methane flames in atmospheric condition. *Energy* 45:669–675. <https://doi.org/10.1016/j.energy.2012.07.027>
- Shang R, Zhang Y, Zhu M et al. (2016) Laminar flame speed of CO<sub>2</sub> and N<sub>2</sub> diluted H<sub>2</sub>/CO/air flames. *International Journal of Hydrogen Energy* 41:15056–15067. <https://doi.org/10.1016/j.ijhydene.2016.05.064>
- R.J. Kee, J.F. Grcar, M.D. Smooke, J.A. Miller (1985) PREMIX: Report No. SAND85-8240
- Kee R, Rupley F, Miller J (1989) Chemkin-II: A Fortran chemical kinetics package for the analysis of gas-phase chemical kinetics
- Blanquart G (2015) Effects of spin contamination on estimating bond dissociation energies of polycyclic aromatic hydrocarbons. *CalTech 2.3. Int J Quantum Chem* 115:796–801. <https://doi.org/10.1002/qua.24904>
- G.P. Smith, D.M. Golden, M. Frenklach, N.W. Moriarty, B. Eiteneer, M. Goldenberg, C.T. Bowman, R.K. Hanson, S. Song, W.C. Gardiner, V.V. Lissianski, Z. Qin GRI\_Mech. GRI\_Mech 3.3. <http://combustion.berkeley.edu/gri-mech/version30/text30.html>
- Appel J, Bockhorn H, Frenklach M (2000) Kinetic modeling of soot formation with detailed chemistry and physics: laminar premixed flames of C<sub>2</sub> hydrocarbons. *ABF. Combustion and Flame* 121:122–136. [https://doi.org/10.1016/S0010-2180\(99\)00135-2](https://doi.org/10.1016/S0010-2180(99)00135-2)
- Hai Wang, Xiaoping You, Ameya V. Joshi, Scott G. Davis, Alexander Laskin, Fokion Egolopoulos & Chung K. Law USC II detailed mechanism. USC II Mech Version II. [http://ignis.usc.edu/Mechanisms/USC-Mech%20II/USC\\_Mech%20II.htm](http://ignis.usc.edu/Mechanisms/USC-Mech%20II/USC_Mech%20II.htm)
- Kathrotia T, Richter S, Naumann C et al. (2018) Reaction Model Development for Synthetic Jet Fuels: Surrogate Fuels As a Flexible Tool to Predict Their Performance. DLR -89 species, 1327 reactions. In: Volume 3: Coal, Biomass, and Alternative Fuels; Cycle Innovations; Electric Power; Industrial and Cogeneration; Organic Rankine Cycle Power Systems. DLR. American Society of Mechanical Engineers
- Reuter CB, Zhang R, Yehia OR et al. (2018) Counterflow flame experiments and chemical kinetic modeling of dimethyl ether/methane mixtures. *HPMech 3.3. Combustion and Flame* 196:1–10. <https://doi.org/10.1016/j.combustflame.2018.06.004>
- G.P. Smith, Y.Tao, H. Wang (2016) Foundational Fuel Chemistry Model Version 1.0 (FFCM-1). FFCM-1. <https://web.stanford.edu/group/haiwanglab/FFCM1/pages/release-notes.html>
- Metcalfe WK, Burke SM, Ahmed SS et al. (2013) A Hierarchical and Comparative Kinetic Modeling Study of C<sub>1</sub> – C<sub>2</sub> Hydrocarbon and Oxygenated Fuels. *Aramco. Int J Chem Kinet* 45:638–675. <https://doi.org/10.1002/kin.20802>
- Günther R (1984) *Verbrennung und Feuerungen*, Unveränd. Nachdr. [d. Ausg. Berlin, Heidelberg, New York, Springer, 1974]. Springer, Berlin
- Wu Y, Modica V, Rossow B et al. (2016) Effects of pressure and preheating temperature on the laminar flame speed of methane/air and acetone/air mixtures. *Fuel* 185:577–588. <https://doi.org/10.1016/j.fuel.2016.07.110>